Neuron, Vol. 15, 181–191, July, 1995, Copyright © 1995 by Cell Press

Desensitized States Prolong $GABA_A$ Channel Responses to Brief Agonist Pulses

Mathew V. Jones and Gary L. Westbrook
Vollum Institute
and Department of Neurology
Oregon Health Sciences University
Portland, Oregon 97201

Summary

We studied the role of desensitization at inhibitory synapses by comparing nonequilibrium $GABA_A$ channel gating with inhibitory postsynaptic currents (IPSCs). Currents activated by brief pulses of 1–10 mM GABA to outside-out patches from cultured hippocampal neurons mimicked GABA-mediated IPSCs. Although the average open time of single $GABA_A$ channels following brief pulses was less than 10 ms, channels entered long (τ = 38–69 ms) closed states and subsequently reopened. Movement through these states resulted in paired-pulse desensitization. The time required for deactivation after removal of agonist also increased in proportion to the extent of desensitization. These results suggest that visits to desensitized states buffer the channel in bound conformations and underlie the expression of long-lasting components of the IPSC. Reopening after $GABA_A$ receptor desensitization may thus enhance inhibitory synaptic transmission by prolonging the response to a brief synaptic GABA transient.

Introduction

γ-aminobutyric acid type A ($GABA_A$) receptor–mediated inhibitory postsynaptic currents (IPSCs) peak rapidly (0.5–5 ms) and usually decay with two time constants ranging from a few milliseconds to tens or hundreds of milliseconds (Edwards et al., 1990; Pearce, 1993; Jones and Harrison, 1993; Puia et al., 1994; Borst et al., 1994). No consensus has been reached as to the factors responsible for the multiphasic decay or the duration of IPSCs. These issues have important consequences because the IPSC decay determines the time course of the resistive shunt and hyperpolarization that prevent neuronal firing in response to excitatory inputs. For example, prolongation of the IPSC decay is thought to be responsible for the therapeutic effects of sedative benzodiazepines and most general anesthetics (Tanelian et al., 1993; Franks and Lieb, 1994), whereas disinhibition produces effects ranging from anxiety to seizure activity (Haefely, 1989; Worms and Lloyd, 1981).

$GABA_A$ receptors have a relatively low affinity for GABA (10–20 μM) (Akaike et al., 1985; Bormann and Clapham, 1985; Maconochie et al., 1994) and display brief openings and bursts (0.2–25 ms) in steady-state single-channel studies (Bormann and Clapham, 1985; Weiss and Magleby, 1989; Macdonald et al., 1989; Twyman et al., 1990). Assuming a brief free GABA transient in the synaptic cleft, these properties predict an IPSC decay of no more than 10–25 ms, much shorter than is frequently observed. This discrepancy could indicate that the GABA transient is not brief. Alternatively, synaptically activated channels may visit desensitized states that are difficult to characterize in steady-state single-channel records (Colquhoun and Hawkes, 1983; Macdonald and Twyman, 1992; Maconochie et al., 1994). Therefore, to understand $GABA_A$ channel gating as it occurs at the synapse, we analyzed gating under nonequilibrium conditions using rapid agonist application to outside-out patches from cultured hippocampal neurons. The ensemble average of patch currents evoked by short (1–10 ms) GABA pulses decayed with biexponential kinetics similar to the IPSC. Single-channel gating under these conditions included frequent visits to long desensitized states, followed by reopening. Use of paired pulses with low and high affinity agonists and fitting of the currents to a kinetic model showed that channel reopening after desensitization can account for the decay of patch currents. We propose that rapidly equilibrating desensitized states prolong the $GABA_A$-mediated IPSC and provide a mechanism for low affinity receptors to support long-lasting synaptic currents.

Results

Our basic strategy in probing the factors responsible for shaping the IPSC was to isolate the contribution of channel kinetics using excised membrane patches and rapid agonist application techniques. We then compared responses in patches with IPSCs and also with responses predicted by a simple kinetic model. In some figures, simulated currents are superimposed on the experimental responses to illustrate the performance of the model. Finally, we used predictions of the model to reconcile the results of steady-state and nonstationary studies of $GABA_A$ channel gating with the kinetics of inhibitory synaptic currents.

IPSCs and $GABA_A$ Receptor Responses

$GABA_A$ receptor currents in outside-out patches of cultured hippocampal neurons were evoked using a piezoelectric translator to make rapid switches (<2 ms 10%–90% solution exchange time) between control and agonist-containing solutions (see Experimental Procedures). In each patch experiment, a series of trials separated by >5 s was used to generate an ensemble average (patch current). Figure 1 illustrates a comparison between an autaptically evoked IPSC and the patch current evoked by a 5 ms pulse of 1 mM GABA. Both the IPSC and patch current decay were well fit by the sum of two exponentials (IPSC: τ_{fast} = 50 ± 30 ms [64% ± 11% of amplitude], τ_{slow} = 171 ± 92 ms, n = 4; patches, 1–10 mM GABA, 1–10 ms: τ_{fast} = 29 ± 12 ms [58% ± 9%], τ_{slow} = 254 ± 85 ms, n = 13). There was no significant difference between IPSCs and patch currents ($p(\tau_{fast})$ = 0.26; $p(amp_{fast})$ = 0.45; $p(\tau_{slow})$ = 0.18). The similarity of these responses suggests that a brief GABA transient at the

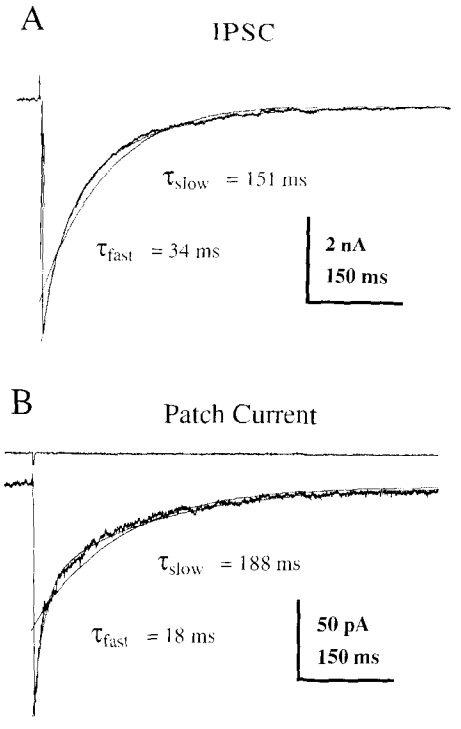

Figure 1. IPSCs and GABA-Activated Patch Currents Have Similar Time Courses

(A) A biexponential fit (superimposed on the current) adequately described the IPSC decay (τ_{fast} = 34 ms [57% of amplitude], τ_{slow} = 151 ms). The closest (but inadequate) monoexponential fit (τ = 101 ms) is also shown. IPSCs were autaptically evoked by 5 ms steps from −60 to +60 mV at 20 s intervals. The Na^+ spike artifact has been omitted. Bath application of 100 μM bicuculline methiodide completely blocked the IPSCs (n = 2; data not shown).

(B) Patch currents were accurately described by a biexponential function (τ_{fast} = 18 ms [53%], τ_{slow} = 188 ms, superimposed), but not by a single exponential (τ = 136 ms, superimposed). The duration of GABA application is shown by the open tip current (top trace). Bicuculline methiodide (100 μM) blocked patch responses by 90% ± 6% (n = 5; data not shown).

synapse is sufficient to produce long-lasting biphasic currents.

A rough estimate of the peak synaptic GABA concentration was obtained by comparing the rise rate of the IPSC (347 ± 141 s^{-1}; n = 3 cells) with that of patch currents. The plot of patch current rise rate (10%–90% rise $time^{-1}$) versus concentration saturated at 1420 s^{-1}, with an EC_{50} of 1.6 mM (legend to Figure 2A). The interpolated peak concentration in the cleft is 527 μM, similar to the estimate of Maconochie et al. (1994). Assuming that GABA is present long enough for channels to reach their maximum open probability, this estimate represents a lower limit, because IPSCs can be slowed by cable filtering or asynchronous GABA release.

There are several possible mechanisms for the biphasic decay of the IPSC. Edwards et al. (1990) and Pearce (1993) suggested that kinetically distinct receptor subtypes underlie the fast and slow components. One interpretation of the IPSC decay is that fast components are mediated by rapidly unbinding (low affinity) receptors, whereas slow components are due to slowly unbinding (high affinity) receptors (e.g., Colquhoun et al., 1977; Lester and Jahr, 1992; Pan et al., 1993). This notion predicts that the fast component should be small at low GABA concentrations and increase with increasing concentration. We observed just the opposite, as shown in Figure 2. The rise rates of patch currents increased as GABA was increased from low (10 μM) to high (10 mM) concentrations (Figure 2A). The fast component of decay, however, was significantly larger and faster at 10 μM than at 10 mM (Figures 2B and 2C). Therefore, the biphasic decay observed in our experiments cannot be explained simply on the basis of two populations of channels with different affinities. The larger slow component at high concentrations is more consistent with models in which multiliganded channels spend more time in conducting states overall than do monoliganded channels (Macdonald et al., 1989; Twyman et al., 1990; Busch and Sakmann, 1990).

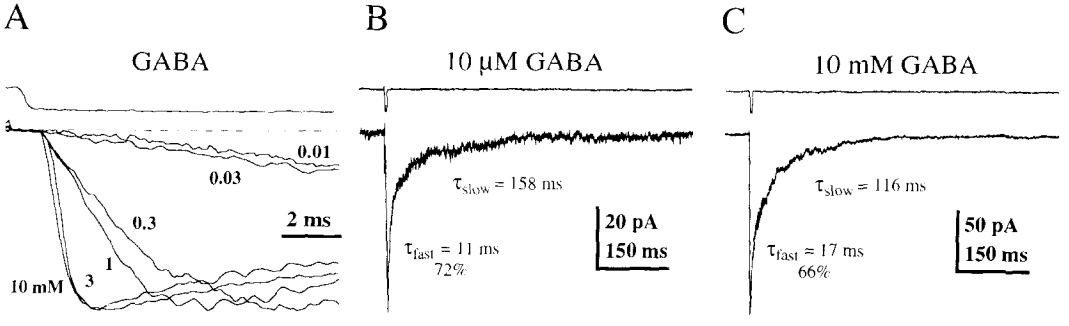

Figure 2. Patch Current Activation and Deactivation Depend on GABA Concentration

(A) Patch current activation was faster at high GABA concentrations. GABA (0.01–10 mM) was applied for 400 ms. Traces are normalized currents from different patches (n ≥ 4 at each concentration). The plot of the current rise rate vs. concentration was fit to the equation R = 1/Rise time = $(R_{max}[GABA])/(EC_{50} + [GABA])$. R_{max} was 1420 s^{-1} and EC_{50} was 1.6 mM. The open tip currents (top) often preceded the patch currents (bottom) by several hundred microseconds, perhaps owing to differences in solution exchange rates between the patch and open tip.

(B) A low GABA concentration pulse (10 μM, 5 ms) evoked a large fast component of deactivation. The parameters of deactivation in this patch are shown next to the trace. In four patches, τ_{fast} was 15 ± 4 ms (77% ± 4%) and τ_{slow} was 240 ± 81 ms.

(C) The slow component of deactivation was more pronounced at high GABA concentrations (1 mM, 5 ms). In 13 patches (1–10 ms pulses, 1–10 mM GABA), τ_{fast} was 29 ± 12 ms (58% ± 8%) and τ_{slow} was 254 ± 93 ms. The fast decay phase was significantly larger and faster for 10 μM than 1 mM GABA ($p < .003$).

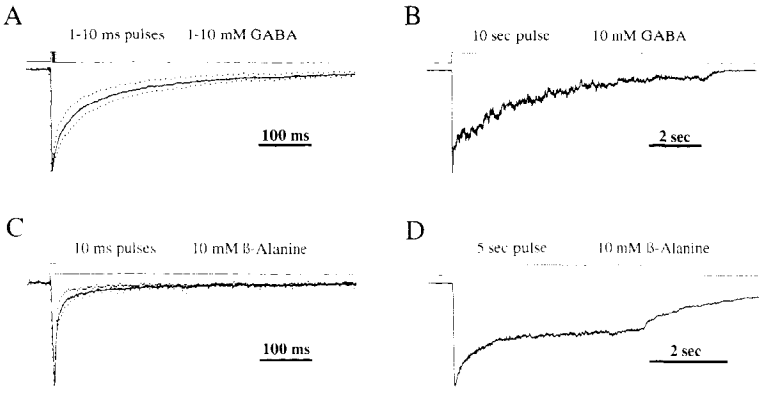

Figure 3. Deactivation and Desensitization of Currents Activated by GABA and β-Alanine.

(A and C) Currents activated by short pulses of high GABA and β-alanine concentrations were normalized. Point-by-point means (solid traces) and standard deviations (dotted traces) were calculated for 13 GABA patches and 11 β-alanine patches. β-alanine produced a significantly faster decay time constant and larger fast component than GABA (β-alanine: τ_{fast} = 7 ± 2 ms [81% ± 11% of amplitude], τ_{slow} = 132 ± 64 ms, n = 11, $p \leq 0.0006$, as compared with GABA; see legend to Figure 2C). The pulse duration is illustrated schematically.

(B and D) Desensitization to long pulses of GABA (10 s) and β-alanine (5 s) was described as the sum of two exponential functions and a constant term describing the steady-state current level. For GABA (n = 4), τ_{fast} was 81 ± 40 ms (26% ± 6% of total amplitude) and τ_{slow} was 1868 ± 755 ms. For β-alanine (n = 3), τ_{fast} was 80 ± 60 ms (32 ± 9%) and τ_{slow} was 947 ± 520 ms. The extent of desensitization at steady state was greater for GABA (90% ± 4%) than for β-alanine (59% ± 17%).

Agonist-Specific Kinetics

Although receptor affinity considerations alone cannot account for the current decay after short pulses, the unbinding rate must ultimately contribute to the relaxation from activated states back toward unbound states (deactivation). To examine the relative contributions of binding, unbinding, and other kinetic parameters, we compared currents activated by GABA and β-alanine, which differ by 250-fold in EC_{50} (GABA, ~20 μM; β-alanine, ~5 mM; Jones, Dzubay, and Westbrook, unpublished data). Current decay was significantly faster after short pulses of β-alanine than after GABA (Figures 3A and 3C), consistent with a faster unbinding rate for β-alanine. The rise rates of β-alanine currents (307 ± 52 s^{-1}, 10 mM, 5 ms, n = 11) were also more than 3-fold slower than those of GABA currents under similar conditions (988 ± 376 s^{-1}, 1–10 mM, 1–10 ms pooled, n = 13), suggesting that β-alanine also has a slower binding rate. The combination of slower binding and faster unbinding predicts that, for a given concentration, β-alanine will occupy fewer binding sites than GABA. Therefore, kinetic behaviors that arise from multiliganded states will be less pronounced for β-alanine. This is consistent with the failure of β-alanine to evoke large slow components of deactivation. Desensitization during long applications of β-alanine was also less complete than for GABA (Figures 3B and 3D). The accumulation of channels in desensitized states may therefore be related to the degree of receptor occupancy.

β-alanine and GABA currents arose from similar channels because both were blocked by 100 μM bicuculline methiodide (1–10 ms pulses, 1–10 mM, GABA: 90% ± 6%, n = 5; β-alanine: 98% ± 1.5%, n = 4), deactivated with two exponential components, and desensitized with two exponential components. Although we cannot exclude the possibility that GABA and β-alanine produce different open probabilities or microscopic desensitization rates, in

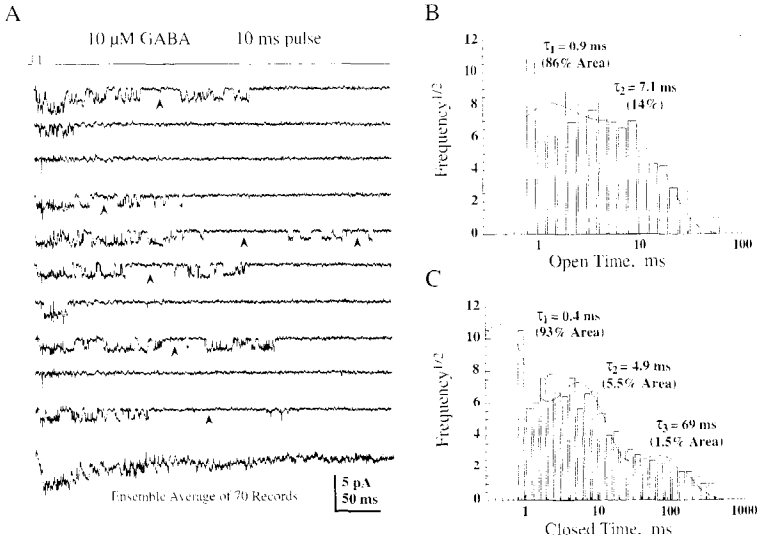

Figure 4. Channel Kinetics Underlying Macroscopic Deactivation

(A) Consecutive records and an ensemble average of single-channel currents activated by brief GABA pulses (shown schematically at the top). The mean inward channel currents were 1.7 pA at −60 mV (28 pS), although occasional subconductance openings to 1.3 pA were observed. The arrowheads indicate long closures (>25 ms) followed by reopenings. Inward piezoelectric artifacts (e.g., third trace from the top) were excluded from the analysis. The ensemble average of 70 records had a two component deactivation with τ_{fast} = 56 ms (68%) and τ_{slow} = 247 ms. Note that individual openings are much shorter than the decay of the ensemble average. Similar results were obtained in four other patches.

(B and C) Open and closed time histograms are from the patch shown in (A). The last closure in each record was ignored, resulting in a total of 856 events for both open and closed time histograms. Fitting was performed over the bin range displayed.

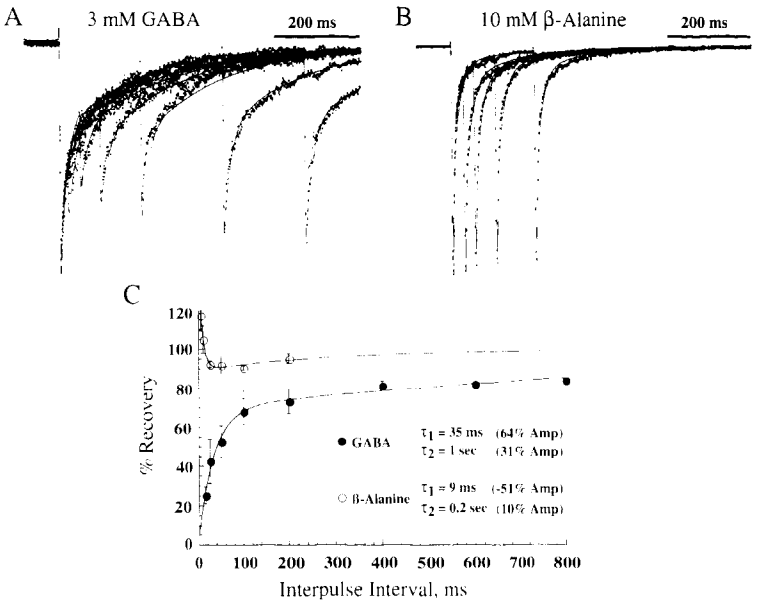

Figure 5. Short Pulse Desensitization Occurs with GABA, but Not with β-Alanine

(A) Pairs of GABA pulses (3 mM, 1 ms) were given at 25, 50, 100, 200, 400, and 600 ms intervals. The second response in each pair was reduced at short interpulse intervals. Ten trials separated by 20 s were interleaved, averaged, and normalized to the first response. Dotted lines are patch currents, and the solid lines are simulated paired-pulse responses generated by the kinetic model, using the parameters for GABA in Figure 7.

(B) Paired pulses of β-alanine produced little desensitization. Interpulse intervals were 25, 50, 100, and 200 ms. Solid lines are simulations using the parameters for β-alanine in Figure 7.

(C) The percentage recovery from desensitization ([Peak2 − Onset]/[Peak1 − Onset] × 100) is plotted as a function of interpulse interval (IPI). Peak1 and Peak2 are the amplitudes of the first and second response in a pair and Onset is the current just before the start of the second response. Results for GABA (closed circles; n = 3) and β-alanine (open circles; n = 4) are shown as mean ± SEM. The solid lines are fits to the equation

$$\% \text{ Recovery} = 100 - \Sigma a_i \exp(-\text{IPI}/\tau_i)$$

where τ_i and a_i are the time constant and amplitude of component i. More than 100% of the first current amplitude is available at short interpulse intervals for β-alanine, because the receptors are not fully saturated even at 10 mM (Jones, Dzubay, and Westbrook, unpublished data).

later sections we will show that binding and unbinding rates alone are sufficient to account for differences among agonists.

Underlying Channel Kinetics

To gain a better understanding of the rate-limiting steps in channel gating that govern macroscopic current decay, we measured the open and closed dwell times of single channels in response to brief (1–10 ms) pulses of 10–30 μM GABA (Figure 4). We were able to estimate upper limits for open times and lower limits for closed times, despite the presence of rare multiple channel openings. Figure 4A shows ten consecutive individual records and an ensemble average from one patch, along with the corresponding dwell time histograms. The measured channel open times of 0.9 and 7.1 ms (Figure 4B) were much too short to account for the ensemble time constants of 56 and 247 ms for this patch (see also Figure 2B). Thus, although there were on average 12.2 openings per application (in the patch shown), closed periods must be a major factor in shaping deactivation after brief pulses.

The closed times showed a complex distribution, with a long duration component of 69 ms in this patch (Figure 4C). Maconochie et al. (1994) also observed long closures during deactivation of patch currents. In five patches, such long closures appeared 384 times in 280 records and had an average lifetime of 44 ± 3 ms (mean ± SEM; range, 38–69 ms). $GABA_A$ channels therefore had a high probability of entering a long-lived closed state after binding GABA and a high probability of leaving that state to open again before unbinding. This long bound closed state may represent one of the states underlying the macroscopic desensitization seen during long pulses of GABA or β-alanine. Although we did not obtain sufficiently long data sets to perform burst or cluster analyses, the long closures we observed during deactivation after short GABA pulses may also correspond to the gaps used to identify bursts or clusters in steady-state experiments (see below and Colquhoun and Hawkes, 1982; Bormann and Clapham, 1985; Twyman et al., 1990).

Short Pulse Desensitization and Recovery

If a short GABA pulse is sufficient to drive channels into a long bound closed state, then desensitization should be apparent in ensemble averages or macroscopic currents. Paired pulse experiments confirmed this prediction (Figure 5). When pairs of 1–3 ms GABA pulses were given at variable intervals, the second pulse evoked a smaller peak current than the first pulse, demonstrating that channels did not return to the unbound state immediately after closing, but rather entered an agonist-insensitive closed (i.e., desensitized) state. Channels recovered from short pulse desensitization with biexponential kinetics (Figures 5A and 5C, closed circles). When pairs of longer GABA pulses (5 s) were given, the second response was strongly depressed and recovered with a time constant of 13 s (n = 4; data not shown). GABA thus promoted entry into a rapidly entered and exited desensitized state, as well as a slowly entered and exited state. In contrast, β-alanine produced notable macroscopic desensitization during long pulses (see Figure 3D), but not during pairs of short pulses (Figures 5B and 5C, open circles). These results suggest that

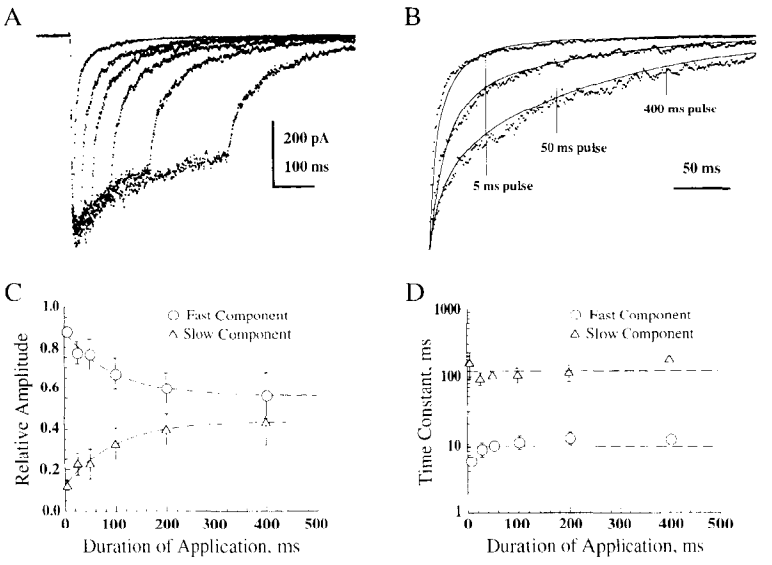

Figure 6. Long Agonist Exposure Causes Desensitization and Prolongs Deactivation

(A and B) Currents were activated by 5, 50, 100, 200, and 400 ms pulses of 10 mM β-alanine. Trials were interleaved in order of increasing pulse duration and were separated by 20 s intervals. Each trace is the average of 10 trials. In (B), deactivation of selected traces from (A) were normalized to the current at the end of the agonist pulse. Note that deactivation became longer as the pulse duration was increased. The solid lines are simulations of the deactivation currents for each pulse duration, using the kinetic model and parameters for β-alanine in Figure 7.

(C) The relative amplitudes of fast (circles) and slow (triangles) components of deactivation from three patches (mean ± SEM) are plotted as a function of pulse duration. The dashed lines are fits to the equation $([A_0 - A_\infty]\exp[-t/\tau] + A_\infty)$, where t is the pulse duration. A_0 and A_∞ are the amplitudes at t = 0 and at infinity, respectively. Note that the slow component increases and the fast component decreases with increasing pulse duration. The states producing the fast and slow components can be approximated as a two-state system, with an interconversion time constant (τ) of 95 ± 25 ms.

(D) The time constants from the currents fitted in (C) are plotted as a function of pulse duration. The dashed lines are the mean time constants (9.5 and 116 ms). Unlike the relative amplitudes, the time constants of deactivation were unaffected by the pulse duration.

after a brief pulse, GABA occupies receptors long enough for many channels to accumulate in desensitized states, whereas β-alanine does not.

Desensitization Prolongs Deactivation

As GABA produces both greater desensitization and slower deactivation than β-alanine, it is possible that desensitization and the slow decay component are mechanistically related. We tested this hypothesis by varying the duration of β-alanine pulses and examining the decay of currents after the agonist was removed. Figures 6A and 6B shows that the duration of deactivation increased as the pulse duration (and the extent of desensitization) increased. Fitting of deactivation currents revealed that the prolongation was due to an increase in the relative amplitude of the slow component (Figure 6C), but that the time constants were unchanged (Figure 6D). These data indicate that channels accumulate in slowly deactivating states as they are desensitizing, consistent with the idea that slow deactivation is directly related to the entry and subsequent exit from desensitized states.

A Model of Deactivation

To examine the role that desensitization may play in shaping patch current deactivation and IPSCs, we developed a model of GABA$_A$ channel gating (Figure 7A; see Experimental Procedures). This model is structurally similar to previous models (Macdonald et al., 1989; Busch and Sakmann, 1990) but incorporates desensitized states that were required to account for our experimental data. The model features two sequential GABA binding steps. Monoliganded receptors ($Bound_1$) can enter a brief open state ($Open_1$) and a very long desensitized state (D_{slow}), whereas doubly liganded receptors ($Bound_2$) can enter a longer open state ($Open_2$) and a rapidly equilibrating desensitized state (D_{fast}). The opening (β_1, β_2) and closing rates (α_1, α_2) were fixed based on the measured open and closed dwell time constants (see Figure 4), whereas the binding (k_{on}), unbinding (k_{off}), desensitization (d_1, d_2), and resensitization (r_1, r_2) rates were chosen by varying parameters until good fits to macroscopic currents were achieved (see Experimental Procedures).

We first tested the ability of the model to fit our experimental data. Using the final rates given in Figure 7B, the model reproduced the biexponential deactivation in response to single and paired pulses of GABA and β-alanine (see Figures 5A and 5B, solid lines) and also the deactivation time course in response to increasing pulse durations of β-alanine (see Figure 6). An important quantitative prediction of the model is that the dwell time in D_{fast} should be between 40 and 67 ms, which closely matches the long closed time of individual channels (38–69 ms; see Figure 4C). Our model is therefore able to account for both the observed macroscopic currents and single-channel gating.

More generally, the model predicts that GABA$_A$ current deactivation is shaped by a precise balance between microscopic desensitization, resensitization, and unbinding rates. Using simulated 1 ms pulses of saturating agonist concentrations, we examined the effects of varying these microscopic rates on the movement of channels through open states and D_{fast} (Figure 8). Reducing the unbinding rate from 600 s^{-1} (the value predicted for β-alanine) to 100 s^{-1} (the value for GABA) prolongs the time-dependent open probability by increasing the slower decay components (Figure 8A$_1$), and also increases the number of channels in D_{fast} (Figure 8A$_2$). The dependence of D_{fast} on the unbinding rate explains why paired-pulse desensitization is agonist specific. In addition, the fast phase of decay (Figure 8A$_1$)

A

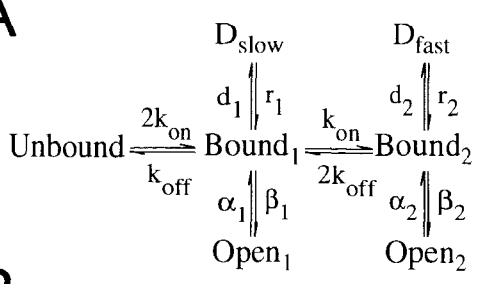

B

Constant	GABA	β-alanine
k_{on} ($\mu M^{-1}s^{-1}$)	3	0.015
k_{off} (s^{-1})	150	450-800
β_1 (s^{-1})	200	200
α_1 (s^{-1})	1111	1111
β_2 (s^{-1})	2500	2500
α_2 (s^{-1})	142	142
d_1 (s^{-1})	13	13
r_1 (s^{-1})	0.13	0.13
d_2(s^{-1})	750-1000	750-1000
r_2 (s^{-1})	15-25	15-25
$P_{o\,(max)}$	0.6-0.8	0.6-0.8

Figure 7. A Quantitative Model of $GABA_A$ Channel Gating

(A) A Markov model featuring two agonist binding steps, each providing access to open and desensitized states, reproduces the main features of nonstationary channel gating observed in our experiments.

(B) Alterations in the binding and unbinding rates alone are sufficient to account for the different kinetics produced by GABA and β-alanine. See Results and Experimental Procedures for the methods used to determine the structure and rate constants of the model.

coincides with the accumulation of channels in D_{fast} (Figure 8A_2), whereas the slow phase coincides with the emptying of D_{fast}.

The model predicts that both the entry and exit rates of D_{fast} are critical in shaping macroscopic deactivation. D_{fast} was best fit with an entry rate (d_2) of 750–1000 s^{-1} and an exit rate (r_2) of 15–25 s^{-1}. Reducing the entry rate into D_{fast} shortens rather than prolongs the total duration of current (Figure 8B), whereas excessively short (5 ms, r_2 = 200 s^{-1}) or long (100 ms, r_2 = 0.1 s^{-1}) dwell times in D_{fast} both reduce the effective current duration (Figure 8C). A slow unbinding rate therefore allows channels to remain bound long enough to access D_{fast}, where they are retained temporarily before reopening.

Discussion

Our results suggest that a synaptic GABA transient reaching ~500 μM and lasting a few milliseconds is sufficient to produce the kinetics of IPSCs recorded from cultured hippocampal neurons. In response to such a GABA transient, channels frequently enter a desensitized state and then reopen. This behavior suggests that the peak open probability and duration of the fast decay component are limited by fast desensitization, and that the slow component is produced by reopening after exit from desensitized states. This mechanism effectively redistributes $GABA_A$-mediated inhibition over hundreds of milliseconds.

Limitations of the Nonstationary Kinetic Approach

Our interpretations depend on the adequacy of our model in predicting channel gating at the synapse, and on the assumption that synaptic $GABA_A$ channels are kinetically similar to those in outside-out patches. Macroscopic patch responses to brief glutamate pulses have provided an excellent model of glutamate-mediated EPSCs (Trussell and Fischbach, 1989; Colquhoun et al., 1992; Lester and Jahr, 1992), even though patch excision can modify some aspects of nicotinic acetylcholine (nACh) and N-methyl-D-aspartate channel kinetics (e.g., Trautmann and Siegelbaum, 1983; Covarrubias and Steinbach, 1990; Lester and Jahr, 1992; Lester et al., 1993). Similarly, brief pulses of GABA produce currents that mimic IPSCs (Maconochie et al., 1994; Puia et al., 1994; this study).

Our experiments were designed to emphasize deactivation and desensitization, which are behaviors of the bound channel. The analysis therefore does not provide detailed information about the rates, number, and cooperativity of binding reactions. These parameters are not critical to our interpretations, but their measurement will provide a quantitative test of our predictions concerning monoliganded receptors and the 200-fold slower binding rate of β-alanine relative to GABA. We modeled the synaptic GABA transient as a square pulse that reaches all activatable channels simultaneously. This appears to be a reasonable approximation, as currents in both patch and modeling experiments were insensitive to changes in pulse duration between 1 and 10 ms. Therefore, factors that affect the precise shape of the effective free GABA transient, such as multivesicular release or diffusion across the receptor array, may not contribute greatly to IPSC decay kinetics. Furthermore, we do not expect monoliganded openings to be important in shaping individual IPSCs, as our model predicts that less than 4% of the total charge passes through $Open_1$ in response to a 1 ms pulse of 100 μM GABA. Our conclusions concerning the insensitivity to the shape of the GABA transient and the contribution of monoliganded receptors contrast with those of Busch and Sakmann (1990), who did not include desensitization in their model. Although our model captures many features of both macroscopic and single $GABA_A$ channel properties, it is not necessarily unique. For example, D_{fast} could proceed from an open state or require binding of additional GABA. The major qualitative result remains that desensitized states can play an important role in shaping $GABA_A$ current deactivation.

Variation among $GABA_A$ Receptors

Although the composition of native $GABA_A$ receptors is not known, many subunits have been cloned and are differ-

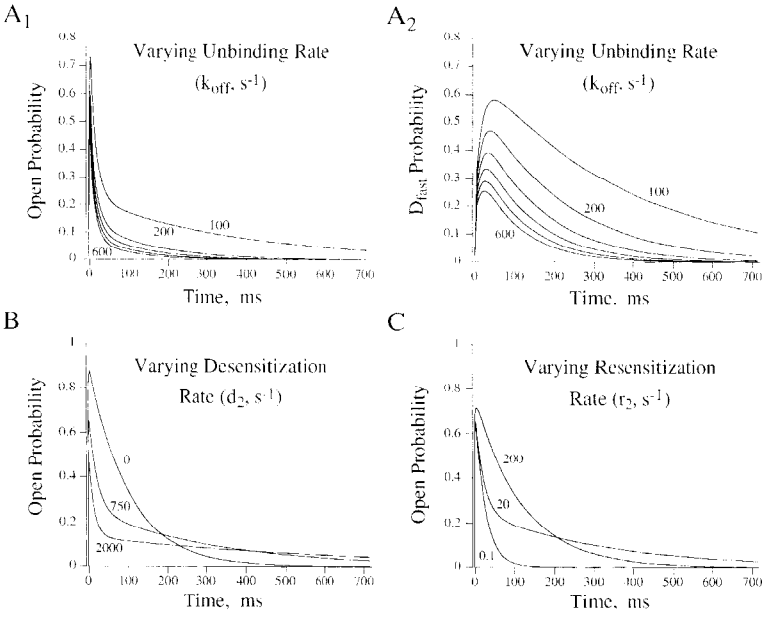

Figure 8. Both Unbinding and Desensitization Can Shape Deactivation

(A_1 and A_2) The model parameters in Figure 7 were used to examine the effects of varying the unbinding rate on Open Probability (Open1 + Open2) and occupancy of D_{fast} (k_{off} = 100, 200, 300, 400, 500, and 600 s^{-1}). Slower unbinding rates produced slower deactivation (A_1) and greater desensitization (A_2).

(B) Reducing the fast desensitization rate (d_2) increased the initial peak current (Open Probability), but reduced the total current duration.

(C) Expression of a distinct slow phase of deactivation occurred only over a specific range of exit rates from D_{fast} (r_2 given next to each trace).

entially expressed in the hippocampus during development (Wisden et al., 1992; Laurie et al., 1992; Fritschy et al., 1994). Three subunit combinations potentially present in hippocampal neurons exhibit biexponential deactivation when expressed in HEK293 cells (Verdoorn, 1994), demonstrating that relatively homogenous receptor populations often produce complex kinetics (Verdoorn et al., 1990; Angelotti and Macdonald, 1993; Celentano and Wong, 1994; Verdoorn, 1994). It is reasonable to expect that the receptors we studied were not structurally identical, but our data were well described by a model that assumes a kinetically homogenous channel population. Differences in IPSC kinetics between preparations may, however, be due to different $GABA_A$ receptor isoforms or to posttranslational modification. For example, Puia et al. (1994) recently showed that Purkinje cells have substantially faster IPSC decay and patch current deactivation than cerebellar granule cells. The faster Purkinje cell responses could be due to faster agonist unbinding (e.g., Figure 8A_1) or to slower exit from desensitized states (e.g., Figure 8C). These two possibilities could be distinguished using paired-pulse experiments. Alteration of these microscopic parameters may therefore be an important functional consequence of the structural variety or modulation of $GABA_A$ receptors. In support of this hypothesis, we have recently acquired evidence that modulation of desensitization can alter the kinetics of both patch currents and IPSCs (Jones and Westbrook, 1994).

Bursts, Clusters, and Macroscopic Currents

The fine structure of microscopic $GABA_A$ channel kinetics has been revealed by single-channel studies using steady-state GABA application (Bormann and Clapham, 1985; Weiss and Magleby, 1989; Weiss, 1988; Twyman et al., 1990; Newland et al., 1991). In such studies, channel openings may be grouped into bursts and clusters separated by critical gaps (Colquhoun and Hawkes, 1982). The gap for defining bursts is often 5–10 ms at 1–10 μM GABA (Bormann and Clapham, 1985; Twyman et al., 1990). However, because the number of channels in a patch is rarely known, it is not easy to determine whether a long closed time component represents the dissociation of agonist or a bound desensitized state. It has therefore been difficult to define kinetic rates governing desensitization and affinity or to place the observed burst and cluster components within the context of IPSCs (Macdonald and Twyman, 1992).

We used Q matrix simulations (Colquhoun and Hawkes, 1982; see Experimental Procedures) to predict the hierarchy in which openings are grouped into bursts and clusters and compared these predictions with the steady-state behavior observed by others. The results of simulations using the model and the median rates from Figures 7A and 7B are summarized in Table 1. At equilibrium, the frequencies of bursts and durations of clusters were greater at higher GABA concentrations, as expected owing to shifting of the equilibrium away from Unbound and D_{slow}. Average burst durations (10–15 ms) in these simulations were quite close to the average values found in adrenal chromaffin cells (12.8 ms; Bormann and Clapham, 1985) and spinal cord neurons (10.3 ms; Twyman et al., 1990). A comparison of the predicted peak and equilibrium dose–response curves revealed that receptors appeared to be of higher affinity after desensitization (peak: $P_{o(max)}$ = ~0.6, EC_{50} = 16 μM, n = 1.9; steady state: $P_{o(max)}$ = ~0.3, EC_{50} = 2.7 μM, n = 1.7, where n is the Hill coefficient). Predictions of slow relaxations and steady-state kinetics can be further improved by allowing a slow transition between D_{fast} and D_{slow}, although this method was not employed here. Surprisingly, our simulations also predict that at low GABA concentrations channels spend most of their agonist-bound time in D_{slow}. Small or slow GABA transients should produce pronounced long-lasting desensitization and a low P_o, whereas large and fast transients should bypass D_{slow}. Monoliganded desensitized states may therefore act as a high pass filter to attenuate the response to slowly

Table 1. Single-Channel Properties of the Kinetic Model

Condition	Number of Openings	Time Open (%)	Number of Visits to D_{fast}	Duration (ms)	Bound Time (%)[a]	Bound Time in D_{fast} (%)[b]	Time Bound in D_{slow} (%)[c]
Equilibrium (1 μM GABA)					81	0.4	98
per burst	1.3	27	NA	10			
per cluster	1.4	22	0.1	13			
Equilibrium (10 μM GABA)					98	2.9	94
per burst	1.8	59	NA	15			
per cluster	2.5	29	0.5	43			
Equilibrium (10 mM GABA)					99.5	66	~0
per burst	2.9	83	NA	26			
per cluster	2049	29	733	56,000			
Deactivation from $Bound_2$ (0 μM GABA)					29[d]	15[d]	6.7[d]
per burst	2.5	76	NA	22[e]			
per cluster	9	28	2.8	231[e]			

Data is from Q matrix simulations of ~1000 s records. NA, not applicable.
[a] (Total time bound)/(Total time simulated) × 100.
[b] (Total time in D_{fast})/(Total time bound) × 100.
[c] (Total time in D_{slow})/(Total time bound) × 100.
[d] During a 1024 ms long sweep.
[e] Corresponds to a macroscopic decay time constant.

rising GABA transients due to spillover of GABA from distant synapses (Isaacson et al., 1993).

In simulated deactivation from the $Bound_2$ state, channels visited D_{fast} approximately once for every three times that they opened and remained there ~20 times longer than in either open state. The ensemble average of sweeps containing at least one visit to D_{fast} (72% of all sweeps) produced a biexponential deactivation (τ_{fast} = 16 ms [54% amplitude]; τ_{slow} = 254 ms), as compared with the monoexponential deactivation (τ = 28 ms) of sweeps lacking a visit to D_{fast}. The sum of these two ensemble averages (τ_{fast} = 21 ms [67% amplitude]; τ_{slow} = 253 ms) suggests that the single-channel burst (22 ms) and cluster (231 ms) durations approximate the fast and slow components of deactivation, respectively. These values are in close agreement with the average components of patch current deactivation (τ_{fast} = 29 ms [58% amplitude]; τ_{slow} = 254 ms) and are within 1 SD of the IPSC component values (τ_{fast} = 50 ms [64% amplitude]; τ_{slow} = 171 ms). Visits to D_{fast} can therefore organize deactivation kinetics by spacing bursts to produce long-lasting and multiphasic currents.

The Physical Basis of Desensitization

Our data suggest that desensitization maintains the channel within a set of states that have a high probability of reopening before the agonist can dissociate. This situation is in many ways analogous to that produced by sequential channel blockers. For example, open channel block of nACh receptors can add slow components to end-plate current decay, because the time spent in blocked states adds to the normal burst duration (Beam, 1976; Neher and Steinbach, 1978). This is similar to the role we postulate for D_{fast} in adding to the cluster duration of $GABA_A$ channels. A desensitized state is formally equivalent to a blocked state with a fixed blocker concentration. We speculate that a common physical basis may underlie this formal equivalence. For the nACh and 5HT3 receptors, mutation of single conserved amino acid residues in the suspected pore-forming regions dramatically reduce some forms of desensitization (Revah et al., 1991; Yakel et al., 1993). This may also be true for a Drosophila $GABA_A$ receptor (ffrench-Constant et al., 1993). It is possible that these residues themselves may interfere with conduction (Revah et al., 1991) or serve as receptors for a blocking particle. Such a blocking particle cannot, however, be the agonist itself, as free agonist was removed before long duration closures were observed (see Figure 4A).

Multiple Purposes of Desensitization at Synapses

Desensitization has evolved in ligand-gated channels from several phylogenetically distinct families (e.g., Katz and Thesleff, 1957; Trussell and Fischbach, 1989; Mayer et al., 1989; Sather et al., 1990; Legendre et al., 1993; Akaike and Kaneda, 1989; Yakel et al., 1993; Valera et al., 1994; Brake et al., 1994), suggesting that it confers an important adaptive advantage. Conversely, desensitization kinetics vary among channel types, suggesting a variety of functions. The specific contribution of desensitization to synaptic transmission can be evaluated with paired-pulse experiments. For example, desensitization of nACh channels is slow relative to deactivation and may not affect the shape of synaptic currents, but rather limit the response frequency at which receptors follow presynaptic signals (Magleby and Palotta, 1981; Franke et al., 1991). For AMPA channels, rapid desensitization with slow recovery may shorten synaptic currents and severely limit the response frequency (Trussell and Fischbach, 1989; Trussell et al., 1993; Raman and Trussell, 1995). Our results for $GABA_A$ channels, and those of Lester and Jahr (1992) for N-methyl-D-aspartate channels, show that strong desensitization that recovers over the course of deactivation can limit the response frequency, but also prolong synaptic currents. Desensitization therefore appears to be a versa-

tile mechanism for tailoring channel kinetics to the requirements of individual synapses through the balance between desensitization, resensitization, and unbinding rates.

Experimental Procedures

Neuron Culture

Hippocampal neurons from 1- to 3-day-old Sprague-Dawley rats were grown either in monolayer cultures (Forsythe and Westbrook, 1988) or on microdot islands as described by Bekkers and Stevens (1991). Recordings were performed 1–3 weeks after plating. No electrophysiological differences between the two culture conditions were observed.

Data Acquisition and Analysis

Recordings were made using Sylgard-dipped (Dow-Corning, Midland, MI) fire-polished borosilicate glass pipettes containing 144 mM CsCl, 1 mM $CaCl_2$, 3.45 mM BAPTA, 10 mM HEPES, 5 mM Mg_2ATP (pH 7.2 and 315 mOsmol). The extracellular solution contained 140 mM NaCl, 2.8 mM KCl, 1 mM $MgCl_2$, 1.5 mM $CaCl_2$, 10 mM HEPES, 10 mM D-glucose (pH 7.4 and adjusted to 325 mOsmol with sucrose). For whole-cell recordings, cesium was replaced by potassium, and 5 μM 6-cyano-7-nitroquinoxaline-2,3-dione was added to the extracellular solution. In β-alanine experiments, 1 μM strychnine was also added.

Cells and patches were voltage clamped at −60 mV (Axopatch 1B, Axon Instruments, Foster City, CA) and continuously perfused with extracellular solutions via 50–400 μm ID local perfusion pipes. The recording chamber was also perfused at ~2 ml/min. Currents were filtered at 1–2 kHz and sampled at 10 kHz. Recurrent synaptic responses (autaptic IPSCs) were evoked using 1–5 ms voltage steps to +60 mV. Rapid solution exchange was accomplished as previously described (Lester and Jahr, 1992), and 10%–90% exchange times less than 2 ms were confirmed at the end of each patch experiment by monitoring the change in liquid junction potential at the pipette tip after patch rupture. Patch currents and IPSCs represent the average of five or more trials.

Data were acquired using AxoBASIC and analyzed off-line with AxoBASIC or AxoGraph (Axon Instruments). Single-channel gating was studied using 10–30 μM GABA to minimize overlapping events. Channel events were detected and collated by a home-written program, using a 50% threshold crossing criterion (based on a 28 pS conductance) and a 400 ms minimum event duration. Accurate detection was monitored by inspection of ideal records superimposed on the raw data by the detection program. The final closure in each record was excluded from detection, but the first closure (first latency) was included, no corrections were made for missed events, and the rare simultaneous openings were included. Log-binning (Sigworth and Sine, 1987) and least squares fitting of histograms were performed using Excel (Microsoft, Redmond, WA) and Kaleidograph (Synergy, Reading, PA). The number of components was incremented until either the area of additional components was less than 1% of the total area or until new components became dominated by single bins. Long closures (>9.8 ms) were defined by the method of equal proportions of misclassifications (Colquhoun and Sakmann, 1985) based on the closed time distribution (see Figure 4). Whole-cell currents were fit using a Chebyshev algorithm. The number of exponential components was initially determined by eye and checked by comparing the sum of squared errors for fits of one, two, and three exponents. In a small number of experiments, addition of a low amplitude third component improved the fit. For comparisons between experiments, however, we regularly used the best two-component fit.

Kinetic Modeling

Macroscopic current modeling was performed using SCoP (Simulation Resources, Berrien Springs, MI). The model included two equal and independent GABA binding steps and monoliganded openings, consistent with results from single-channel studies (Macdonald et al., 1989; Twyman et al., 1990; Macdonald and Twyman, 1992). The single-channel gating for five patches was examined to determine opening and closing rates. The values for the patch with the lowest channel activity (see Figure 4) provided the best approximation of the values for a one channel patch. We observed two open states ($Open_1$ and $Open_2$) and fixed their closing (α) and opening rates (β) using the inverse open and closed dwell time constants, respectively. Two desensitized states (D_{fast} and D_{slow}) were included based on the biexponential desensitization and recovery patterns (see Figures 3C and 3D; see Figure 5). The maximum open probability ($P_{o(max)}$) was derived from nonstationary variance analysis (Sigworth, 1980; Jones and Westbrook, unpublished data). Our $P_{o(max)}$ values are in agreement with those from intraburst single-channel measurements (Newland et al., 1991). The binding (k_{on}), unbinding (k_{off}), desensitization (d_1, d_2), and resensitization (r_1, r_2) rates given in Figure 7B are the optimal values (or the extreme limits, always with less than 2-fold variation) for producing good fits to experimental data by eye.

For Q matrix simulations (Colquhoun and Hawkes, 1982), Q and Π matrices were calculated from the model and the median values in Figure 7B. From an initial state, a pair of computer-generated random numbers (q and p) were used to choose the exit path (from Π) and the dwell time (from Q). The present state and dwell time were then recorded, and calculations were repeated for the next state. In a 100 s test simulation, $q \cong p = 0.497 \pm 0.29$ ($n = 3057$) and $p = 9 \times 10^{-5}q + 0.5$, confirming that q and p were indeed random and uncorrelated (Miller, 1981). At low GABA concentrations, the theoretical mean dwell times in Unbound, D_{slow}, and D_{fast} were all greater than 10 ms, and entry into any of these states was therefore defined as a critical gap for terminating a burst (Bormann and Clapham, 1985; Macdonald et al., 1989; Twyman et al., 1990). Entry into Unbound or D_{slow} also ended a cluster. This approach is the inverse of that normally taken with experimental data, in which the duration of a closure is known but the state to which it corresponds is not. Equilibrium simulations (1000 s) were run at 1 and 10 μM GABA, and nonequilibrium relaxations (976 sweeps of 1024 ms) were studied by starting each sweep in $Bound_2$ at 0 μM GABA to simulate patch current deactivation after a brief saturating GABA pulse.

Data are presented as mean ± SD throughout unless otherwise noted. Statistical significance was determined using unpaired, two-tailed t tests, assuming unequal variances. Differences were considered significant at the $p \leq 0.05$ level.

Acknowledgments

We thank Jeff Dzubay for assistance with some of the experiments, Jeff Volk for neuron cultures, and Drs. Craig Jahr and John Clements for advice on software and an unending series of helpful discussions. This work was supported by National Institutes of Health grants NS26494 (G. L. W.), T32 DA07262, and F32 NS09716 (M. V. J.).

The costs of publication of this article were defrayed in part by the payment of page charges. This article must therefore be hereby marked *"advertisement"* in accordance with 18 USC Section 1734 solely to indicate this fact.

Received February 3, 1995; revised March 30, 1995.

References

Akaike, N., Hattori, K., Inomata, N., and Oomura, Y. (1985). γ-aminobutyric acid- and pentobarbitone-gated chloride currents in internally perfused frog sensory neurones. J. Physiol. *360*, 367–386.

Akaike, N., and Kaneda, M. (1989). Glycine-gated chloride current in acutely isolated rat hypothalamic neurons. J. Neurophysiol. *62*, 1400–1409.

Angelotti, T. P., and Macdonald, R. L. (1993). Assembly of $GABA_A$ receptor subunits: α1β1 and α1β1γ2s subunits produce unique ion channels with dissimilar single-channel properties. J. Neurosci. *13*, 1429–1440.

Beam, K. G. (1976). A voltage-clamp study of the effect of two lidocaine derivatives on the time course of end-plate currents. J. Physiol. *258*, 279–300.

Bekkers, J. M., and Stevens, C. F. (1991). Excitatory and inhibitory autaptic currents in isolated hippocampal neurons maintained in cell culture. Proc. Natl. Acad. Sci. USA *88*, 7834–7838.

Bormann, J., and Clapham, D. E. (1985). γ-aminobutyric acid receptor channels in adrenal chromaffin cells: a patch-clamp study. Proc. Natl. Acad. Sci. USA *82*, 2168–2172.

Borst, J. G. G., Lodder, J. C., and Kits, K. S. (1994). Large amplitude

variability of GABAergic IPSCs in melanotropes from *Xenopus laevis*: evidence that quantal size differs between synapses. J. Neurophysiol. *71*, 639–655.

Brake, A. J., Wagenbach, M. J., and Julius, D. (1994). New structural motif for ligand-gated ion channels defined by an ionotropic ATP receptor. Nature *371*, 519–523.

Busch, C., and Sakmann, B. (1990). Synaptic transmission in hippocampal neurons: numerical reconstruction of quantal IPSCs. Cold Spring Harbor Symp. Quant. Biol. *55*, 69–80.

Celentano, J. J., and Wong, R. K. S. (1994). Multiphasic desensitization of the $GABA_A$ receptor in outside-out patches. Biophys. J. *66*, 1039–1050.

Colquhoun, D., and Hawkes, A. G. (1982). On the stochastic properties of bursts of single ion channel openings and of clusters of bursts. Phil. Trans. R. Soc. Lond. (B) *300*, 1–59.

Colquhoun, D., and Hawkes, A. G. (1983). The principles of the stochastic interpretation of ion-channel mechanisms. In Single-Channel Recording, B. Sakmann and E. Neher, eds. (New York: Plenum Press), pp. 135–175.

Colquhoun, D., and Sakmann, B. (1985). Fast events in single-channel currents activated by acetylcholine and its analogues at the frog muscle end-plate. J. Physiol. *369*, 501–557.

Colquhoun, D., Large, W. A., and Rang, H. P. (1977). An analysis of the action of a false transmitter at the neuromuscular junction. J. Physiol. *266*, 361–395.

Colquhoun, D., Jonas, P., and Sakmann, B. (1992). Action of brief pulses of glutamate on AMPA/kainate receptors in patches from different neurones of rat hippocampal slices. J. Physiol. *458*, 261–287.

Covarrubias, M., and Steinbach, J. H. (1990). Excision of membrane patches reduces the mean open time of nicotinic acetylcholine receptors. Pflügers Arch. *416*, 385–392.

Edwards, F. A., Konnerth, A., and Sakmann, B. (1990). Quantal analysis of inhibitory synaptic transmission in the dentate gyrus of rat hippocampal slices: a patch-clamp study. J. Physiol. *430*, 213–249.

ffrench-Constant, R. H., Rocheleau, T. A., Steichen, J. C., and Chalmers, A. E. (1993). A point mutation in a Drosophila GABA receptor confers insecticide resistance. Nature *363*, 449–451.

Forsythe, I. D., and Westbrook, G. L. (1988). Slow excitatory postsynaptic currents mediated by N-methyl-D-aspartate receptors on cultured mouse central neurones. J. Physiol. *396*, 515–534.

Franke, C., Hatt, H., and Dudel, J. (1991). Steep concentration dependence and fast desensitization of nicotinic channel currents elicited by acetylcholine pulses, studied in adult vertebrate muscle. Pflügers Arch. *417*, 509–516.

Franks, N. P., and Lieb, W. R. (1994). Molecular and cellular mechanisms of general anesthesia. Nature *367*, 607–614.

Fritschy, J.-M., Paysan, J., Enna, A., and Mohler, H. (1994). Switch in the expression of rat $GABA_A$-receptor subtypes during postnatal development: an immunohistochemical study. J. Neurosci. *14*, 5302–5324.

Haefely, W. E. (1989). Pharmacology of the allosteric modulation of $GABA_A$ receptors by benzodiazepine receptor ligands. In Allosteric Modulation of Amino Acid Receptors: Therapeutic Implications., E. A. Barnard and E. Costa, eds. (New York: Raven Press), pp. 47–69.

Isaacson, J. S., Solis, J. M., and Nicoll, R. A. (1993). Local and diffuse synaptic actions of GABA in the hippocampus. Neuron *10*, 165–175.

Jones, M. V., and Harrison, N. L. (1993). Effects of volatile anesthetics on the kinetics of inhibitory postsynaptic currents in cultured rat hippocampal neurones. J. Neurophysiol. *70*, 1339–1349.

Jones, M. V., and Westbrook, G. L. (1994). Altering $GABA_A$ channel desensitization shortens IPSC duration. Biophys. J. *68*, A2.

Katz, B., and Thesleff, S. (1957). A study of the "desensitization" produced by acetylcholine at the motor end-plate. J. Physiol. *138*, 63–80.

Laurie, D. J., Wisden, W., and Seeburg, P. H. (1992). The distribution of thirteen $GABA_A$ receptor subunit mRNAs in the rat brain. III. Embryonic and postnatal development. J. Neurosci. *12*, 4151–4172.

Legendre, P., Rosenmund, C., and Westbrook, G. L. (1993). Inactivation of NMDA channels in cultured hippocampal neurons by intracellular calcium. J. Neurosci. *13*, 674–684.

Lester, R. A., and Jahr, C. E. (1992). NMDA channel behavior depends on agonist affinity. J. Neurosci. *12*, 635–643.

Lester, R. A., Tong, G., and Jahr, C. E. (1993). Interactions between the glycine and glutamate binding sites of the NMDA receptor. J. Neurosci. *13*, 1088–1096.

Macdonald, R. L., and Twyman, R. E. (1992). Kinetic properties and regulation of $GABA_A$ receptor channels. In Ion Channels, T. Narahashi, eds. (New York: Plenum Press), pp. 315–343.

Macdonald, R. L., Rogers, C. J., and Twyman, R. E. (1989). Kinetic properties of the $GABA_A$ receptor main conductance state of mouse spinal neurones in culture. J. Physiol. *410*, 479–499.

Maconochie, D. J., Zempel, J. M., and Steinbach, J. H. (1994). How quickly can $GABA_A$ receptors open? Neuron *12*, 61–71.

Magleby, K. L., and Palotta, B. S. (1981). A study of desensitization of acetylcholine receptors using nerve-released transmitter in the frog. J. Physiol. *316*, 225–250.

Mayer, M. L., Vyklicky, L., and Clements, J. (1989). Regulation of NMDA receptor desensitization in mouse hippocampal neurons by glycine. Nature *338*, 425–427.

Miller, A. R. (1981). BASIC Programs for Scientists and Engineers. (Berkeley: Sybex), pp. 13–30.

Neher, E., and Steinbach, J. H. (1978). Local anaesthetics transiently block currents through single acetylcholine-receptor channels. J. Physiol. *277*, 153–176.

Newland, C. F., Colquhoun, D., and Cull-Candy, S. G. (1991). Single channels activated by high concentrations of GABA in superior cervical ganglion neurones of the rat. J. Physiol. *432*, 203–233.

Pan, Z. Z., Tong, G., and Jahr, C. E. (1993). A false transmitter at excitatory synapses. Neuron *11*, 85–91.

Pearce, R. A. (1993). Physiological evidence for two distinct $GABA_A$ responses in rat hippocampus. Neuron *10*, 189–200.

Puia, G., Costa, E., and Vicini, S. (1994). Functional diversity of GABA-activated Cl^- currents in Purkinje versus granule neurons in rat cerebellar slices. Neuron *12*, 117–126.

Raman, I. M., and Trussell, L. O. (1995). The mechanism of α-amino-3-hydroxy-5-methyl-4-isoxazolepropionate receptor desensitization after removal of glutamate. Biophys. J. *68*, 137–146.

Revah, F., Bertrand, D., Galzi, J.-L., Devillers-Thiery, A., Mulle, C., Hussy, N., Bertrand, S., Ballivet, M., and Changeux, J.-P. (1991). Mutations in the channel domain alter desensitization of a neuronal nicotinic receptor. Nature *353*, 846–849.

Sather, W., Johnson, J. W., Henderson, G., and Ascher, P. (1990). Glycine-insensitive desensitization of NMDA responses in cultured mouse embryonic neurons. Neuron *4*, 725–731.

Sigworth, F. J. (1980). The variance of sodium current fluctuations at the node of Ranvier. J. Physiol. *307*, 97–129.

Sigworth, F. J., and Sine, S. M. (1987). Data transformations for improved display and fitting of single-channel dwell time histograms. Biophys. J. *52*, 1047–1054.

Tanelian, D. L., Kosek, P., Mody, I., and MacIver, M. B. (1993). The role of the $GABA_A$ receptor/chloride channel complex in anesthesia. Anesthesiology *78*, 757–776.

Trautmann, A., and Siegelbaum, S. A. (1983). The influence of membrane patch isolation on single acetylcholine-channel current in rat myotubes. In Single Channel Recording, B. Sakmann and E. Neher, eds. (New York: Plenum Press), pp. 473–480.

Trussell, L. O., and Fischbach, G. D. (1989). Glutamate receptor desensitization and its role in synaptic transmission. Neuron *3*, 209–218.

Trussell, L. O., Zhang, S., and Raman, I. M. (1993). Desensitization of AMPA receptors upon multiquantal neurotransmitter release. Neuron *10*, 1185–1196.

Twyman, R. E., Rogers, C. J., and Macdonald, R. L. (1990). Intraburst kinetic properties of the $GABA_A$ receptor main conductance state of mouse spinal chord neurons in culture. J. Physiol. *423*, 193–220.

Valera, S., Hussy, N., Evans, R. J., Adami, N., North, R. A., Surprenant,

A., and Buell, G. (1994). A new class of ligand-gated ion channel defined by P_{2X} receptor for extracellular ATP. Nature *371*, 516–519.

Verdoorn, T. A. (1994). Formation of heteromeric $GABA_A$ receptors containing two different alpha subunits. Mol. Pharmacol. *45*, 475–480.

Verdoorn, T. A., Draguhn, A., Ymer, S., Seeburg, P. H., and Sakmann, B. (1990). Functional properties of recombinant rat $GABA_A$ receptors depend on subunit composition. Neuron *4*, 919–928.

Weiss, D. S. (1988). Membrane potential modulates the activation of GABA-gated channels. J. Neurophysiol. *59*, 514–527.

Weiss, D. S., and Magleby, K. L. (1989). Gating scheme for single GABA-activated Cl^- channels determined from stability plots, dwell-time distributions, and adjacent-interval durations. J. Neurosci. *9*, 1314–1324.

Wisden, W., Laurie, D. J., Monyer, H., and Seeburg, P. H. (1992). The distribution of 13 $GABA_A$ receptor subunit mRNAs in the rat Brain. I. Telencephalon, diencephalon, mesencephalon. J. Neurosci. *12*, 1040–1062.

Worms, P., and Lloyd, K. G. (1981). Functional alterations of GABA synapses in relation to seizures. In Neurotransmitters, Seizures, and Epilepsy, P. L. Morselli, K. G. Lloyd, W. Loscher, B. Meldrum, and E. H. Reynolds, eds. (New York: Raven Press), pp. 37–48.

Yakel, J. L., Lagrutta, A., Adelman, J. P., and North, R. A. (1993). Single amino acid substitution affects desensitization of the 5-hydroxytryptamine type 3 receptor expressed in Xenopus oocytes. Proc. Natl. Acad. Sci. USA *90*, 5030–5033.